Journal of Constructional Steel Research

Volume 118, March 2016, Pages 231–242

Fragility curves for typical steel frames with semi-rigid saddle connections

Amir Kiani , Babak Mansouri , Abdolreza S. Moghadam

Show more

doi:10.1016/j.jcsr.2015.11.001

Highlights

- Traditional steel structures with semi-rigid connections are severely vulnerable to earthquake loads
- For the 2% probability of exceedance in 50 years case, the probability of exceeding the CP performance limit is 90%, 74% and 56% for the 3-story structure consisting of unbraced frames with masonry infill, braced frames with concentric braces and braced frames with masonry infill, respectively.
- The corresponding values (for the 2% probability of exceedance in 50 years case) for the 5-story models are 94%, 69% and 62%.
- These alarming high values suggest that the seismic retrofit of such existing structures is of crucial importance.

Abstract

Steel structures with “saddle” type beam–column connections represent a popular construction practice in Iran. In the present paper, the seismic performance and the vulnerability of such structures are investigated. The seismic responses of three-story and five-story structures are modeled according to the nonlinear incremental dynamic analysis (IDA) procedure considering various frame configurations. Typical frames representing unbraced frames with masonry infill walls, braced frames with concentric bracings and braced frames with masonry infill walls were studied under the effect of 44 real ground motion records. Fragility curves were developed for these structures and the probability of exceedance at immediate occupancy (IO), life safety (LS) and collapse prevention (CP) performance limits was assessed for two seismic hazard scenarios (475 and 2475 years return period). For the 2% probability of exceedance in 50 years case, the probability of exceeding the CP performance limit is 90%, 74% and 56% for the 3-story structure consisting of unbraced frames with masonry infill, braced frames with concentric braces and braced frames with masonry infill, respectively. The corresponding values for the 5-story models are 94%, 69% and 62%. These alarming high values suggest that the seismic retrofit of such existing structures is of crucial importance.

Keywords

Semi-rigid connections; Saddle connections; Masonry infill; IDA; Fragility curves; Performance-based seismic assessment

Fragility Curves for Typical Steel Frames with Semi-Rigid Saddle Connections

Amir Kiani[1], Babak Mansouri[2], Abdolreza S. Moghadam[3]

1- Ph.D. Candidate, International Institute of Earthquake Engineering and Seismology, Tehran, Iran

Tel: +98-21-88655696 **Fax:** +98-21-88884284 **Email:** a.kiani@iiees.ac.ir

2- Assistant Professor, International Institute of Earthquake Engineering and Seismology, Tehran, Iran

Tel: +98-21-22830830 **Fax:** +98-21-22289455 **Email:** mansouri@iiees.ac.ir

Corresponding author's email: mansouri@iiees.ac.ir

3- Assistant Professor, International Institute of Earthquake Engineering and Seismology, Tehran, Iran

Tel: +98-21-22830830 **Fax:** +98-21-22289455 **Email:** moghadam@iiees.ac.ir

Abstract:

In past major earthquakes of Iran, steel structures with a specific type of semi-rigid connections known as the "saddle connection" have proved to be quite vulnerable. Since steel structures with "saddle" connections represent a large number of existing buildings in Iran, their vulnerability assessment seems to be crucial for earthquake mitigation studies. The present paper tries to investigate the performance of such structures and their seismic vulnerability by applying existing fragility assessment procedures. Thus, nonlinear incremental dynamic analysis (IDA) were performed on three- and five-story building models consisting of unbraced frames with masonry infill walls, braced frames with concentric bracings and braced frames with masonry infill walls under the effect of 44 real ground motion records. Then, fragility curves of all models were generated according to the procedures and recommendations outlined in ATC-63 where the performance of each model were assessed for two seismic hazard scenarios including 10% and 2% probability of exceedance in 50 years at immediate occupancy (IO) as well as life safety (LS) and collapse prevention (CP) performance limits. Results indicate that for the 2% probability of exceedance in 50 years scenario, probability of exceeding the CP performance limit is 90%, 74% and 56% for the 3-story models consisting of unbraced frames with masonry infill, braced frames with concentric braces and braced frames with masonry infill, respectively. The corresponding values for the 5-story models are 94%, 69% and 62%. These alarming values suggest that seismic retrofitting of such existing structures is quite essential.

Keywords: Semi-rigid connections; saddle connections; masonry infill; IDA; fragility curves; performance-based seismic assessment.

1. Introduction

In many cities of Iran, due to the relative simplicity in construction as well as relative low construction costs, frames with "saddle" connections have been widely utilized in steel structure constructions. In such frames, continuous parallel beams cross and encase the columns, while the "semi-rigid" connections are formed by two welded angle sections at the top and bottom of each beam. A typical configuration of the connection is shown in Fig. 1. Common lateral load systems of these buildings are masonry infill walls, braces or a combination of both. In past major earthquakes of Iran (e.g. Manjil (Mw. 7.4, 1990) and Bam (Mw. 6.5, 2003), these steel structures showed unsatisfactory performance and in many cases resulted in total structural collapse (Fig. 2).

By referring to the census data of 2006 for Iran [1], a total of 82% of the housing units are recognized as masonry or steel constructions in the whole country. 47.3% of such units have been categorized as low seismic resistant constructions. For Tehran, low quality steel or masonry housing units account for about 50% of the total houses. The key point is that a large number of vulnerable steel structures are those with typical saddle connections as depicted in Fig. 2. It is believed that the assessment of the seismic vulnerability of such structures is central to any "seismic risk reduction" program.

Different studies have been carried out on understanding the seismic behavior and the design of "saddle connection" structures. Moghadam [2] have studied their performance in Manjil earthquake (Mw. 7.4, 1990) and provided recommendations for their retrofit. Amiri et al. [3] studied the seismic performance of such structures using nonlinear static procedure and suggested a method to obtain rigid saddle connections. Their study showed that the enhanced system is capable of providing the "life safety" performance with relatively high safety margin.

Hosseini Hashemi and Hassanzadeh [4] studied a steel saddle frame building with infill panels damaged in the Bam earthquake (Mw. 6.5, 2003) using nonlinear dynamic analysis. They have utilized the recommendations of FEMA-356 [5] for the evaluation process. The results showed good correspondence of the overall behavior of the nonlinear model with the observed response. They concluded that in such complex system, infill panels contribute in preventing the structure from collapse and most of the energy was absorbed and dissipated by them.

Mazrouei et al. [6] proposed a method to retrofit "saddle" connections by adding top and bottom flanges and gusset plates. In their proposed method, a considerable increase in the degree of rigidity of the connection was achieved which resulted in better performance compared with the conventional practice.

In 2011, Shakib et al. [7] investigated the seismic vulnerability and retrofitting of a 19-storey steel building with semi-rigid connections located in the city of Tehran. The results showed that the building was strong enough to resist gravity loads but the strength was not adequate for lateral seismic loadings.

Most of the previous studies have been deterministic, rather than "probabilistic". Due to the random nature of the earthquake shaking, it would be beneficial to study the problem from probabilistic point of view. This paper is an attempt to assess the seismic fragility of such structures in a probabilistic framework. For this purpose, two 3- and 5-story building models with three types of lateral load resisting systems, i.e. unbraced frames with masonry infill walls, braced frames with concentric braces and braced frames with masonry infill walls (6 prototypes in total) have been modeled and subjected to Incremental Dynamic Analysis (IDA) utilizing 44 real ground motions based on the recommendations of ATC-63 (FEMA-P695) [8]. In creating fragility curves, the results obtained from IDA procedure were combined with those of a PSHA for a typical site located in Tehran, and the performance of each model were assessed at immediate occupancy (IO), life safety (LS) and collapse prevention (CP) performance limits. In what follows, the methodology and the results will be provided and discussed in detail.

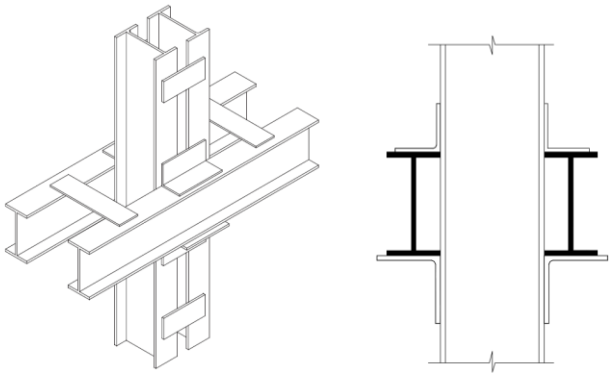

Fig. 1. Typical configuration of Saddle connection

Fig. 2. Brittle saddle connections failure - total collapse examples in Bam earthquake (Mw. 6.5, 2003) [9]

2. Methodology

2.1 General Structural behavior

Previous studies (e.g. [10-12]) have showed that although there is no high rotational rigidity

at the connections (with initial rotational stiffness typically around 900 tonf.m/rad); however, due to the shear and torsional resistance for the connecting angle sections, they are generally categorized as "semi-rigid". Moment-rotation curves for saddle connections has been derived by experimental tests carried out by Karami and Moghadam [10], Mazrouei and Mostafaei [11], Moghadam and Aalaee [12] and Amiri and Aghakouchak [13]. Moghadam and Aalaee [12] provided the moment-rotation curves for six different conventional saddle connections using different beam sections and connection angle sections. They found that the length of the connecting angle sections played major role in the strength of the connection. Also, based on Sadeghian and Moghadam [14] studies, the connection generally cannot exhibit any ductile behavior due to the large stress concentration on the angle welds.

2.2. Typical building configuration

As the first step in this study, as-built drawings of a number of steel frame buildings with saddle connection in the city of Tehran were collected. The collected data provided the typical beam, column and brace sections, connection details as well as the thickness of the infill walls in addition to the overall geometry of the buildings. Based on the collected data, two sets of 3-bay (with typical span length of 5.0 m) frames with 3 and 5 stories (with typical story height of 3.2 m) are considered. Each set includes three variations according to the type of lateral load resisting system; namely unbraced frames with masonry infill walls, braced frames with concentric braces and braced frames with masonry infill walls as depicted in Figs. 3 and 4. In Table 1, some structural specifications of the two model buildings are summarized. For the saddle connections, **L**-10 and **L**-12 angle sections (numbers indicate the leg size in centimeters) with a length of 20 centimeters are used at the top and bottom parts of the connection (see Fig. 1). The dead and live load on the beams are estimated and assumed to be 30 KN/m and 10 KN/m for all typical stories and 30 KN/m and 7.5 KN/m for the roof level, respectively, for typical bay of 5 meters. Additional loading for infill walls were considered to be 7.5 KN/m. Also, steel material is assumed to be of ST-37 type (mild steel) with yield stress equal to 240 MPa. Column bases are considered to be hinged.

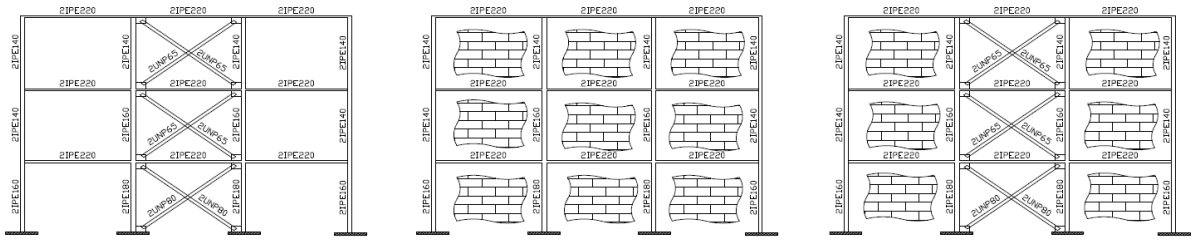

Fig. 3. Schematic view of 3 story building models

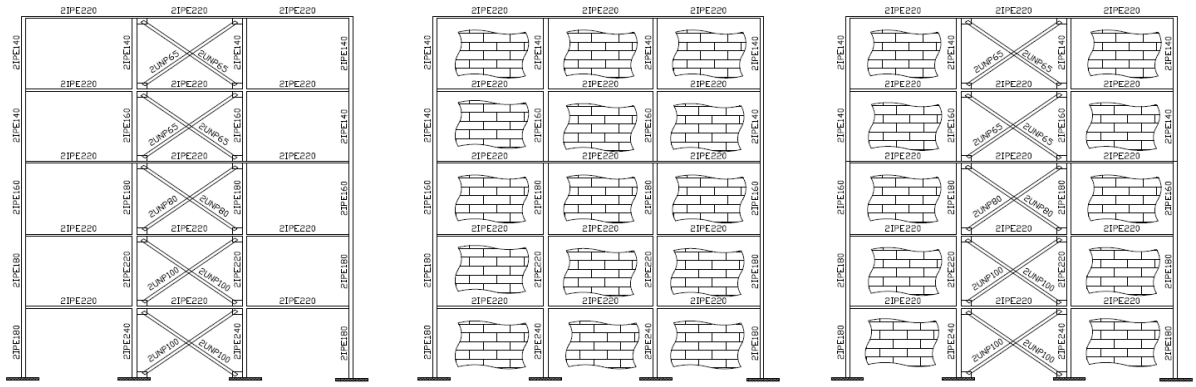

Fig. 4. Schematic view of 5 story building models

Table 1. Detail of sections for different models

No. of Stories	Story	Beams	Interior columns	Exterior columns	Brace Sections	Wall thickness
3 stories	1	IPE220	2IPE180	2IPE160	2UNP80	20 cm
	2	IPE220	2IPE160	2IPE140	2UNP65	20cm
	3	IPE220	2IPE140	2IPE140	2UNP65	20cm
5 stories	1	IPE220	2IPE240	2IPE180	2UNP100	20cm
	2	IPE220	2IPE220	2IPE180	2UNP100	20cm
	3	IPE220	2IPE180	2IPE160	2UNP80	20cm
	4	IPE220	2IPE160	2IPE140	2UNP65	20cm
	5	IPE220	2IPE140	2IPE140	2UNP65	20cm

2.3. Modeling frame elements

For the linear and nonlinear modeling phases, beams, columns and brace sections are modeled as fiber sections. The stress-strain behavior of the fibers is taken as of the mild steel (ST37) with yield strength and yield strain assumed to be 240 MPa and 0.002, respectively. OpenSees [15] computer code was utilized for structural analyses as beams, columns and braces, were considered to behave as “Steel02” material with strain stiffening characteristics based on Giuffré-Menegotto-Pinto Model [16]. Low cycle fatigue effects are also considered in this model. All models were built with nonlinear beam-column elements. Effects associated with the behavior of gusset plates and the in-plane buckling effect for the braces are also taken into account in the modeling process. In the analytical model, all beams and columns are considered as distributed plastic elements with 5 integration points and 20 fibers per section. To consider post buckling behavior of bracing elements, fiber sections were assigned for nonlinear beam-column elements. The bracings are modeled as pinned connection with 1/250 to 1/1000 of the bracing length as in-plane imperfection. For the cyclic analysis, an incremental horizontal displacement history is applied for each in-plane imperfection value [17].

2.4. Modeling saddle connections

Two continuous beams encase each column and this geometry is correctly implemented. Semi-rigid characteristics for the connection are modeled by rotational "zero-length" springs elements (in the OpenSees model) located on each side of the column. Moment-rotation curves for typical saddle connection have been obtained from experimental tests carried out by Moghadam and Aalaee [12] and Amiri and Aghakouchak [13]. The latter provided the moment-rotation curves for six different saddle connections using different beam sections and connection angle sections under cyclic loadings.

For this study, the moment-rotation curve for the most common connection type, namely IPE 240 for the beam sections, and **L-1**0 (10mm thickness) angle section at top and **L**-12 (12mm thickness) angle section at bottom with 20 cm length and medium quality welding as shown in Fig. 5 [13] is utilized in nonlinear modeling of the connections. Since very little test data is available for the hysteretic behavior of such connections, moment-rotation curve of Fig. 5 is considered as the envelop curve for a bilinear hysteresis curve according to the Modified Ibarra Krawinkler Deterioration Model [18].

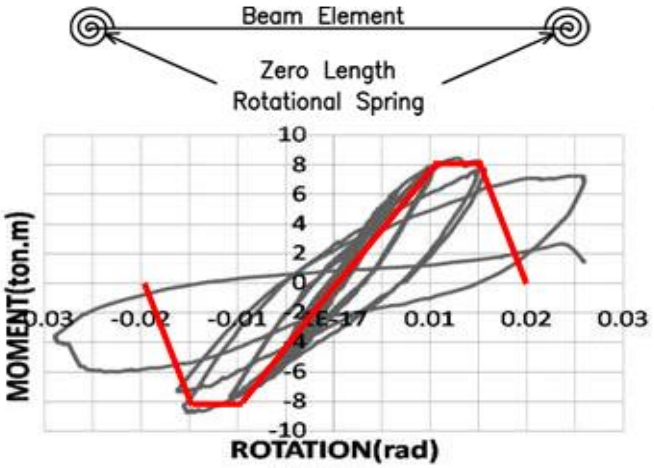

Fig. 5. Moment–rotation curve of saddle connections utilized in this study [13]

2.5. Modeling masonry infill walls

Previous analytical and experimental studies show that infill walls can strongly affect the global stiffness and strength of structural systems [19-21]. Various methods have been proposed in the literature for modeling brick infill walls confined by concrete or steel frames. Mander et al. [19] provided experimental results on the seismic performance of brick-infilled steel frames. Crisafulli et al. [20] investigated and presented different procedures for analysis of infilled walls and discussed the advantages and disadvantages of micro- and macro models. Shing and Mehrabi [21] summarized some of the recent findings and developments on the behavior and modeling relevant to infilled structural systems. Farshchi and Moghadam [22] investigated the behavior of half scale steel braced frames with infill walls by cyclic

loadings tests. According to their results, interaction between the infill and the braces in steel frames may increase stiffness, strength and energy absorption of the whole structural system.

The failure mechanisms of the infill walls are rather complicated. Such mechanism are primarily associated with the horizontal slip, diagonal cracking and corner crushing [20]. In this study, the cyclic behavior of the infill masonry walls are modeled by adopting the hysteresis rules proposed by Crisafulli [23]. This model considers the nonlinear behavior of the masonry infill in compression by a limited hysteretic behavior with pinching effect due to cracked materials. The infills are modeled using two compression struts based on recommendations made by FEMA-356 [5].

Prior to cracking, the lateral rigidity and the elastic in-plane stiffness of a solid unreinforced masonry infill walls shall be represented by the actual infill thickness that is in contact with the frame, t_{inf}, and the diagonal length, r_{inf}, and an equivalent width, a, given by the following equation [5]:

$$a = 0.175(\lambda_I h_{col})^{-0.4} r_{\inf} \tag{1}$$

$$\lambda_I = \sqrt[4]{\frac{E_{me} t_{\inf} \sin 2\theta}{4 E_{fe} I_{col} h_{\inf}}} \tag{2}$$

where,
h_{col} : column height between centerlines of beams in mm,
h_{inf} : height of infill walls in mm,
E_{fe} : expected modulus of elasticity for frame material in MPa,
E_{me} : expected modulus of elasticity of infill material in MPa,
I_{col} : moment of inertia of column in mm^4,
r_{inf} : diagonal length of infill walls in mm,
t_{inf} : thickness of infill walls and equivalent strut in mm, and
θ : angle whose tangent is the infill height-to-length aspect ratio in radians.

$$\theta = \tan^{-1}\left(\frac{h_{\inf}}{L_{\inf}}\right) \tag{3}$$

L_{inf} : length of infill panel, in mm.

Elastic modulus, minimum lower bound for the average compressive strength, limit state strains and also width of struts (Eq.(1) to Eq.(3)) are calculated using empirical recommendations of FEMA-356 [5] as well as the studies conducted by Farshchi and Moghadam [22] and Garivani et al. [24]. The required parameters are summarized in Table 2.

Table 2. Struts mechanical properties

Minimum lower bound of average compressive strength (f_{mcl})	2.0 Mpa
Expected compressive strength (f_{me})	2.4 Mpa
Expected elastic modulus	1320 Mpa
Compressive strain at ultimate strength	0.0020
Ultimate strain	0.0040

In order to model the cyclic behavior of struts in OpenSees software properly, and also to adjust the analytical model with the experimental results, the final parameters (some shown in Table 2) are implemented into the Modified Ibarra-Medina-Krawinkler Deterioration Model [18] with pinched hysteretic response. Based on the Crisafulli model [23] and considering the aforementioned parameters, the hysteretic behavior of struts were derived as shown in Fig. 6(b).

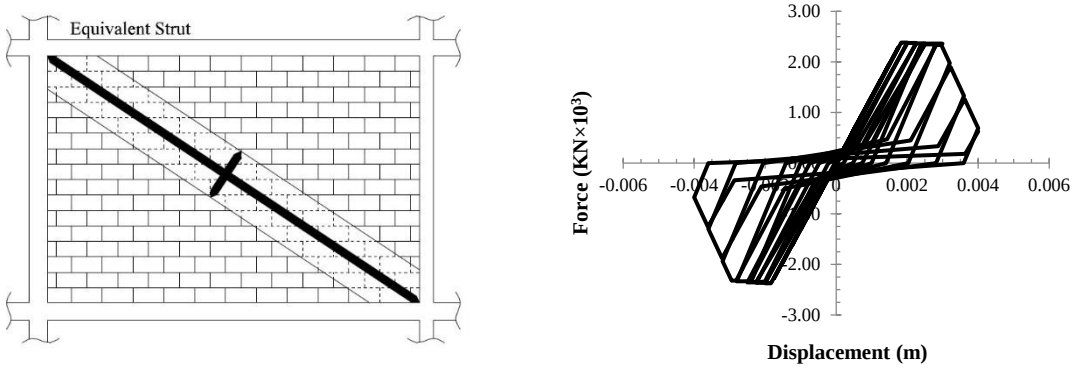

(a) (b)

Fig. 6. (a) Considered strut model for infill walls, (b) Hysteretic behavior of struts by Modified Ibarra-Medina-Krawinkler Deterioration Model

2.6. Analytical model verification

In order to evaluate the adequacy of the analytical model for the braced frame with saddle connections, the half-scale experimental data for a one-story X-CBF (X-type concentrically braced frame) as tested by Veshkini and Aghakouchak [25] has been used. They have tested four two-dimensional braced frames with conventional saddle connections. The authors have used their results to verify the models especially from hysteretic point of view. The hysteresis curves under quasi-static cyclic loading from the above-mentioned study and the ones obtained analytically in this study are overlaid in Fig. 7. It is observed that the model is matched well with the experimental results.

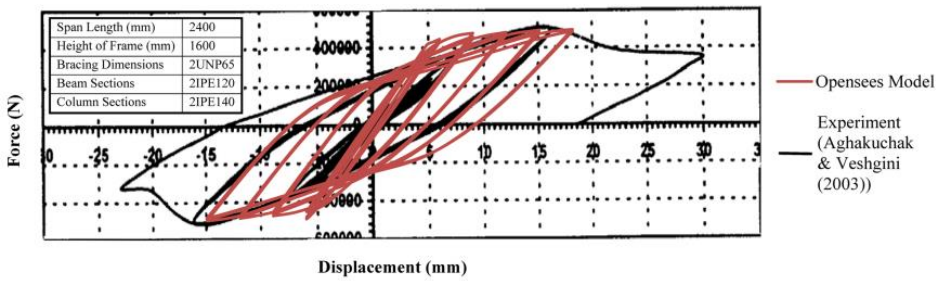

Fig. 7. Structural behavior of experimental results (Veshkini and Aghakouchak [25]) compared with analytical model for "Saddle braced frame"

3. Analysis Procedures and Performance Criteria

3.1. Nonlinear static (pushover) and cyclic analysis

In this section, the static analysis of the considered structural models is discussed. All models are subjected to nonlinear static (pushover) analysis. According to the recommendation of ATC-63, [8] for providing such analysis, all models need to be preloaded by the factored gravity loads combination as:

$$1.05DL + 0.25LL \tag{4}$$

where DL is the dead load and LL is the live load imposed on the structure.

The control node is selected to be at the roof. Distribution of the lateral loading in the pushover analysis is also selected to be as the triangular distribution of story forces in equivalent static seismic loading procedures.

Furthermore in this research, a lateral displacement cycle (positive and negative) of a prescribed amplitude is imposed at the top story. The imposed displacements are applied using a displacement-control integrator, where the load factors are scaled to reach the desired displacement (compared to an imposed-displacement analysis). Performing such an analysis provide a mean to compare the energy dissipation and cyclic strength characteristic of the models.

3.2. Incremental dynamic analysis

Incremental Dynamic Analysis (IDA) is a method to monitor the response of a structural system from the linear elastic phase to their highly nonlinear and even collapse phases under gradually increasing ground motions [26]. Results of such analysis are utilized for generating fragility curves [26]. In order to assess the seismic behavior of the models in this study, the records are scaled continuously. Therefore, the initial and the incremental spectral intensity at first mode of the structures ($S_{a\text{-}T1}$) value are considered as 0.01g and 0.05g respectively. According to ATC-63 [8], the median of spectral intensities of all models need to be scaled to the desired intensity. The corresponding scale-factor should then be applied to all records in the set. The process continues up to any desired intensity level or even to the point of collapse

of the system.

3.2.1. Site characterization, seismic hazard and site-specific spectra

The buildings are located at a high seismic site (51.42E, 35.67N). Site specific spectra has been considered according to uniform hazard spectrum (UHS) method for scaling records for predicting adequate structural responses. Thus results of a recent probabilistic seismic hazard analysis (PSHA) for Tehran region (Gholipour et al. [27]) has been used. Uniform hazard spectra results from PSHA corresponding to 475 and 2475 years return period earthquakes (DBE and MCE spectra) were considered as depicted in Fig. 8.

In extracting these spectra, three NGA (Next Generation of Ground Motion attenuation) models and four GMPEs (Ground Motion Prediction Equations) previously developed by Abrahamson and Silva (1997), Boore et al. (1997), Campbell and Bozorgnia (2003) and Sadigh et al. (1997) have been used by Gholipour et al. [27]. Note that, this site is located on soil type "D" and is located far (greater than or equal to 10 km from assumed fault rupture) from the Rey and North Tehran Faults (with Strike-slip and thrust mechanisms).

Peak ground acceleration for the Maximum Considered Earthquake with 2475 years return period (MCE) is $PGA_{MCE} = 0.875g$ and for Maximum Designed Earthquake with 475 years return period (DBE) is $PGA_{DBE} = 0.37g$.

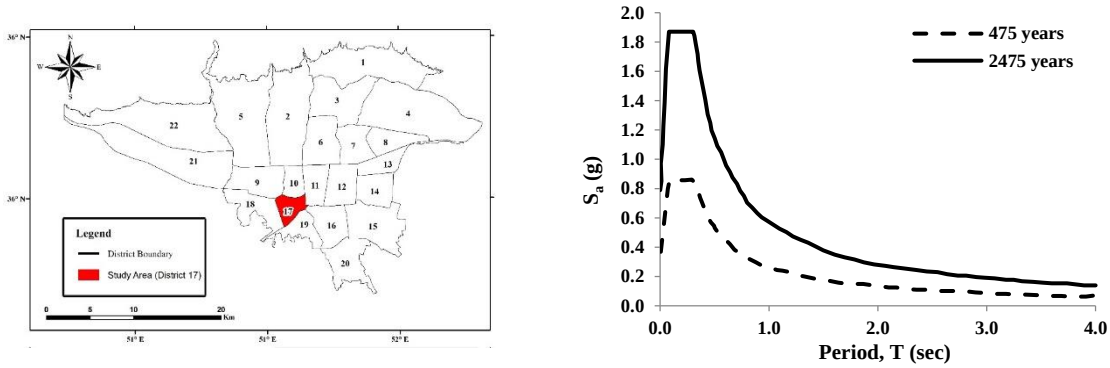

Fig. 8. Uniform hazard spectra generated for the considered site in the city of Tehran

3.2.2. Ground motions selection

Record selection for performing nonlinear time history analyses is a critical issue and many different methods have been developed and used. Shome and Cornell [28] have shown that 10–20 records are usually enough to provide sufficient accuracy in the estimation of seismic demands.

Due to the lack of sufficient medium- to high-intensity earthquake records data in Iran, the authors decided to use the ground motion records of the far-field set of ATC-63 [8]. Thus, in order to perform Incremental Dynamic Analysis (IDA), a set of 44 ground motion records

(recorded at 22 stations with 2 components) as offered by ATC-63 [8] report is selected for investigating the probability of collapse in the site of interest. The set belongs to large magnitudes (M_w=6.5-7.6) and far distances (greater than or equal to 10 km from fault rupture), and includes records from soft rock and stiff soil sites (NEHRP Site Class C and D conditions). They are all from shallow crustal sources (strike-slip and thrust Fault mechanisms). The considered structures of this study are all located on C and D soil type and are regarded as far-field. Thus, it is believed that selection of the records from the ATC-63 [8] set could be consistent. Also, ground motion records were normalized by their peak ground velocities to remove unwarranted variability between records due to inherent differences in event magnitude, source type, the distance to source and site conditions for accurately predicting collapse fragility. 5% damped elastic spectrum of normalized selected records (characteristics are summarized in Table 3) are shown in Fig. 9(a). In Fig. 9(b), the median of the selected ground motion records has been compared with the Design Basis Earthquake (DBE) derived for the site using probabilistic seismic hazard analysis. The comparison confirms that selected records were adequate for the selected site in the city of Tehran.

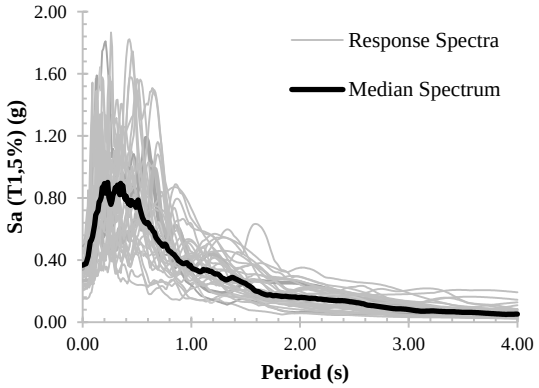

Fig. 9(a). 5% damped elastic spectra of the selected ground motion records with the median spectrum

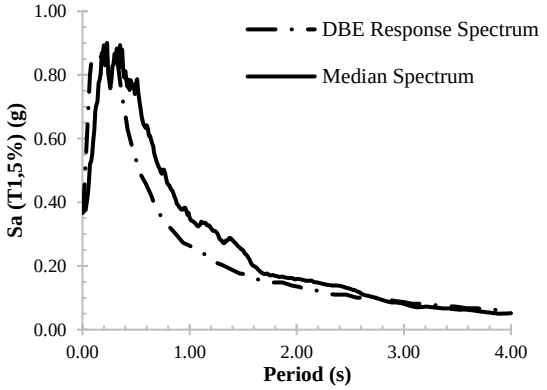

Fig. 9(b). Comparison between median elastic spectra of the selected ground motion records with DBE site-specific spectra (5% damped)

Table 3. Characteristics of the selected ground motion records (ATC-63 [8])

EQ. Name	**PEER-NGA** *Number*	**Duration** *(Sec)*	**Source** *(Fault Type)*	**Soil Type** *NEHRP Class*	**PGA_{max}** *(g)*	**S_a (T=1sec) (g)** *(5% damped)*
Northridge	953	30	Thrust	D	0.42	1.02
					0.52	0.94
Northridge	960	20	Thrust	D	0.41	0.38
					0.48	0.63
Duzce, Turkey	1602	56	Strike-slip	D	0.73	0.72
					0.82	1.16
Hector Mine	1787	45	Strike-slip	C	0.27	0.35
					0.34	0.37
Imperial Valley	169	100	Strike-slip	D	0.24	0.26
					0.35	0.48
Imperial Valley	174	39	Strike-slip	D	0.36	0.24
					0.38	0.23
Kobe, Japan	1111	41	Strike-slip	C	0.51	0.31
					0.50	0.29
Kobe, Japan	1116	41	Strike-slip	D	0.24	0.33
					0.21	0.23
Kocaeli, Turkey	1158	27	Strike-slip	D	0.31	0.43
					0.36	0.61
Kocaeli, Turkey	1148	30	Strike-slip	C	0.22	0.11
					0.15	0.11
Landers	900	44	Strike-slip	D	0.24	0.50
					0.15	0.33
Landers	848	280	Strike-slip	D	0.28	0.20
					0.42	0.36
Loma Prieta	752	40	Strike-slip	D	0.53	0.46
					0.44	0.28
Loma Prieta	767	40	Strike-slip	D	0.56	0.27
					0.37	0.38
Manjil, Iran	1633	53	Strike-slip	C	0.51	0.35
					0.50	0.54
Superstition Hills	721	40	Strike-slip	D	0.36	0.31
					0.26	0.25
Superstition Hills	725	22	Thrust	D	0.45	0.33
					0.30	0.34
Cape Mendocino	829	36	Thrust	D	0.39	0.54
					0.55	0.39
Chi-Chi, Taiwan	1244	90	Thrust	D	0.35	0.49
					0.44	0.95
Chi-Chi, Taiwan	1485	90	Thrust	C	0.47	0.30
					0.51	0.43
San Fernando	68	28	Thrust	D	0.21	0.25
					0.17	0.15
Friuli, Italy	125	36	Thrust	C	0.35	0.25
					0.31	0.30

3.3. Performance criteria and limits

For deriving fragility curves, different damage state limits need to be defined. As suggested by FEMA-350 [29], HAZUS [30] and FEMA-356 [16] among many structural response parameters, the maximum inter-story drift is considered as the primary parameter to evaluate the structural performance. For example, the performance criteria suggested by the HAZUS procedure suggest values for selecting the inter-story drift thresholds relative to four damage states, namely “Slight”, “Moderate”, “Extensive”, and “Complete”. The structures in HAZUS methodology closely related to this study could be regarded as steel braced frame (S2) and steel frame with unreinforced masonry infill walls (S5) buildings.

Experimental results on infill panels obtained by Calvi et al. [31] reveal the response for close-to-collapse limit states (maximum inter-story drift at 1.2 % or larger) and for serviceability limit states (maximum inter-story drift below 0.4%). In some cases, the tests were continued until out of plane expulsion for verifying the ultimate response of the frame alone. In another test experiment, Braz–César et al. [32] indicated that such stiff hybrid frames could withstand a fairly high load until the first cracks appeared in the wall at a drift ratio of around 0.2-0.3%. Thereafter, minor strength and stiffness reduction was observed up to 0.81% drift. The experimental results by Schneider et al. [33] suggested that the contribution of the infill masonry to the strength and stiffness of infilled steel frames was significant up to a drift value of about 1.4%. Beyond this limit, the strength and the stiffness were practically reduced to that of bare steel frame.

In this research, the inter-story drift thresholds for the braced frames and masonry infill walls are taken as those suggested by FEMA-356 [5] recommendation. These values are in good agreement with experimental results as reported by aforementioned studies. For the frames modeled with both steel braces and masonry infill walls, drift ratio ranges relevant to Immediate Occupancy up to about Life Safety, the threshold are assumed similar to that of masonry infill walls as the behavior of the structure is mainly governed by the masonry infills. In larger deformation ranges, the drift is practically controlled by the performance of the bracings as the infill materials have been already crushed and disintegrated. Thus for collapse prevention criteria, the drift ratio thresholds for such frames are taken similar to the frame with bracings only. The above criteria are considered for the modeling as summarized in Table 4.

Table 4. Drift ratio thresholds corresponding to three structural damage states

Building Type	**Drift Ratio at the Threshold of Structural Damage**		
	Immediate Occupancy (IO)	**Life Safety (LS)**	**Collapse Prevention (CP)**
Bracing	0.005	0.015	0.02
Masonry infill wall	0.003	0.006	0.01
Masonry infill wall with bracing	0.003	0.006	0.02

4. Results and Discussions

4.1. Nonlinear static analysis results

For the purpose of performing static nonlinear analysis, inverted triangular distributed lateral load pattern was considered according to code-specified lateral load distribution (Design Static). Fig. 10(a) to Fig. 10(c) show the capacity (pushover) curves of the 3-story frames and Fig. 11(a) to Fig. 11(c) show structural behavior for 3 story frames under cyclic loads.

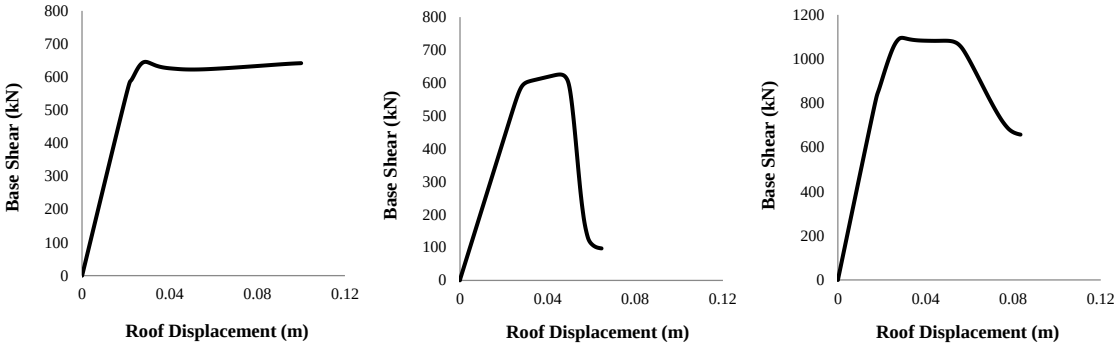

(a) (b) (c)

Fig. 10. Pushover curves for 3 story frame with (a) bracing, (b) infill walls and (c) the combination of bracing and infill walls under inverted triangular lateral load pattern

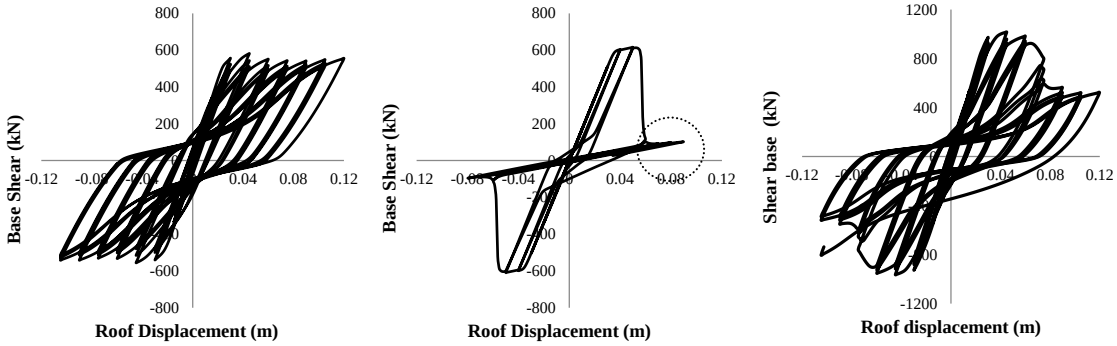

(a) (b) (c)

Fig. 11. Structural behavior for 3 story frame with (a) bracing, (b) infill walls and (c) the combination of bracing and infill walls under cyclic loads

As it can be deduced from Fig. 11, due to the non-ductile behavior of the infill walls, the system is highly affected by their performance. Structure with bare bracings has experienced relatively no major loss in stiffness and strength and the amount of the dissipated energy are as expected. In contrast, frames with infill panels (no bracings) have exhibited much pinching effects with major loss of both stiffness and strength for larger displacements. The encircled region in Fig. 11(b) corresponds to the residual strength and stiffness supplied by the semi-rigid saddle connection which is relatively negligible. It could be concluded that a system with a combination of bracings and infill walls (Fig. 11(c)) experiences two main phases of response up to the point of failure and the resulting hysteresis behavior exhibits a little higher energy dissipation. In the first phase, the behavior is dominated by the stiffness degradation of infill walls. After a quick "transitional" phase, the behavior is similar to the case of the frame merely consisting of the bracings (Fig. 11(a)).

Furthermore, story displacements are plotted for three levels in Fig. 12 for the frames with infills only (without brace elements). Under the incremental cyclic load, due to the equal thickness of the walls in the height of the structure and the higher shear forces at the first

story, the second and the third story displacements are nearly the same and minimal; however, the first story displacement gradually increases with no limitation. This effect explains the soft story formation as illustrated in Fig. 12. The soft-story mechanism is found to be a critical limit state in frames with only infill walls.

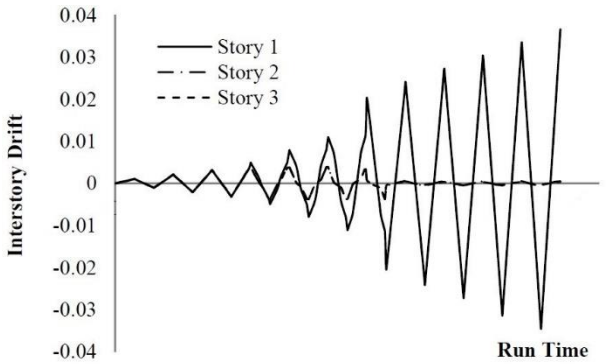

Fig. 12. Formation of soft story in the 3-Story frame with infill walls only

4.2. IDA curves

Incremental dynamic analyses are conducted under a gravity load combination of Eq. (4) and input normalized and scaled ground motions. The normalized records are collectively scaled to a specific ground motion intensity such that the median spectral acceleration of the record set matches the specific-site spectral acceleration at the fundamental period of the model under consideration.

IDA curves are arranged in maximum inter-story drift versus spectral acceleration for each scaled record at the fundamental period of the buildings (Table 5) as shown for three story buildings in Fig. 13.

Table 5. Fundamental periods of considered buildings

No. of Stories	**Lateral Load Resisting System**	**Fundamental Period (sec)**
3	Masonry Infill	0.302
	Bracing	0.294
	Masonry infill with bracing	0.228
5	Masonry Infill	0.474
	Bracing	0.469
	Masonry infill with bracing	0.368

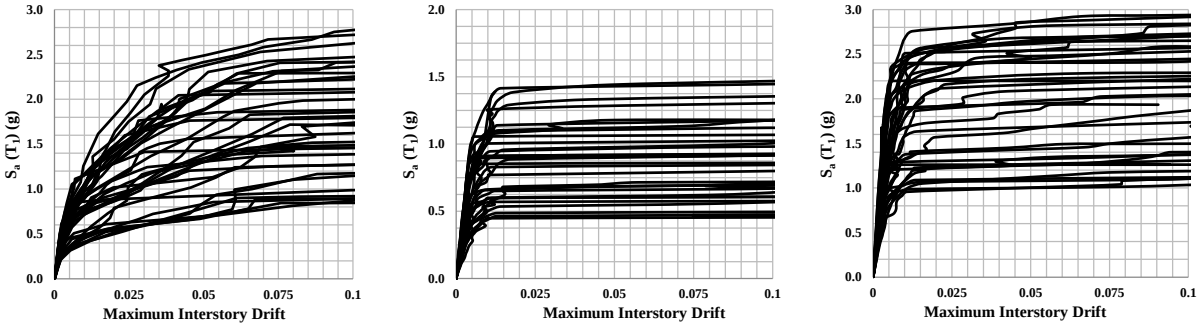

Fig. 13. IDA curves for 3 story steel frame (a) with brace, (b) with infill wall and (c) combination of infill wall and brace

Fig. 13 shows that each curve represents the response of the structure to a single ground motion. The intensity of each ground motion is increased beyond the structural collapse state. The collapse is associated to the conditions where excessive drifts occur under some small increases in the ground motion intensity. As expected, with the increase in the lateral strength of the frames, the demand capacity has increased. Comparing the behavior of frames with infill walls only and frames with bracing only, for low-intensity earthquakes, the relative high stiffness of frames has limited the maximum interstory drifts. Also the braced frame has the additional advantage in increasing the maximum tolerable dynamic drifts as demonstrated from pushover and hysteretic curves.

4.3. Fragility curves development

A "fragility curve" is a measure for evaluating the performance of a particular construction exposed to hazard [26]. Assuming that the data are log-normally distributed, it is possible to develop the fragility curves at desired limit states by computing only the median collapse capacity and logarithmic standard deviation of the IDA results at predefined limit states. The fragility functions then can be analytically calculated using Eq. (5) as adopted in ATC-63 [8] and HAZUS [30]:

$$p[ds \mid S_a] = \Phi\left[\frac{1}{\beta_{\mathrm{RTR}}} \ln\left(\frac{S_a}{S_{a\ 50\%}}\right)\right] \tag{5}$$

Where $S_{a\ 50\%}$ is the median value of spectral acceleration determined from IDA at which the building reaches the threshold of damage state, *ds*, β_{RTR} is the standard deviation of the natural logarithm of spectral acceleration for damage state, *ds*, due to record to record variability in the IDA results, and Φ is the standard normal cumulative distribution function.

In this paper, considering different applied ground motion records, the spectral acceleration for the first mode period of the structure ($S_a\ (T_1)$) and the maximum inter-story drift specific to three damage states (Immediate Occupancy, Life Safety and Collapse

Prevention) are selected as S_a and *ds* values.

Considering IDA results, only the uncertainty due to record-to-record variability (β_{RTR}) is considered explicitly. Therefore it is necessary to modify the developed fragility curves using IDA results to include the uncertainty due to other sources of uncertainty according to ATC-63. The modified fragility curve then can be computed using Eq. (6).

$$p[ds \mid S_a] = \Phi\left[\frac{1}{\beta_{TOT}} \ln\left(\frac{S_a}{S_{a\ 50\%}}\right)\right] \tag{6}$$

Where, β_{TOT} is the total standard deviation of the natural logarithm for each damage state, ds, and modeled by the combination of four contributors to damage variability in Eq. (7).

$$\beta_{TOT} = \sqrt{\beta^2_{RTR} + \beta^2_{DR} + \beta^2_{TD} + \beta^2_{MDL}} \tag{7}$$

Where, β_{RTR}, β_{DR}, β_{TD} and β_{MDL} are Record-to-record uncertainty, design requirements-related uncertainty, test data-related uncertainty and modeling uncertainty, respectively. The effect of each of the aforementioned uncertainties is represented by a lognormal standard deviation parameter. These parameters are evaluated according to ATC-63 in a way that the quality ratings of 'Superior', 'Good', 'Fair' and 'Poor' are translated into quantitative uncertainty values of 0.10, 0.20, 0.35 and 0.50, respectively. In this study β_{RTR} was obtained from the IDA results. Other lognormal standard deviation factors, β_{DR}, β_{TD} and β_{MDR} are assumed respectively equal to 0.35, 0.35 and 0.2.

Through these assumptions the total lognormal standard deviation parameter, β_{TOT}, for the selected building types is calculated and shown in Table 6. In this summarized table, median spectra acceleration ($S_{a\ 50\%}$) are shown together with the lognormal standard deviation associated to record to record variability (β_{RTR}) of IDA.

Highlighting different performance objectives, the derived fragility curves for 3-story and 5-story buildings are shown in Fig. 14 and Fig. 15. In these figures continuous and dashed lines correspond to fragility curves derived from β_{RTR} and β_{TOT}, respectively.

Table 6. Median spectra acceleration and lognormal standard deviation for selected building types

No. of Stories	Building Type	Median Spectral Acceleration (g)			lognormal standard deviation β_{RTR}			lognormal standard deviation β_{TOT}		
		IO	LS	CP	IO	LS	CP	IO	LS	CP
3	Masonry Infill	0.32	0.61	0.78	0.38	0.40	0.39	0.66	0.67	0.66
	Bracing	0.51	0.91	1.17	0.39	0.44	0.48	0.66	0.69	0.72
	Combination of masonry infill and bracing	0.88	1.32	1.69	0.37	0.37	0.42	0.65	0.65	0.68
5	Masonry Infill	0.21	0.44	0.54	0.37	0.40	0.38	0.65	0.67	0.66
	Bracing	0.39	0.64	0.83	0.37	0.42	0.47	0.65	0.68	0.71
	Combination of masonry infill and bracing	0.61	0.91	1.24	0.35	0.38	0.40	0.64	0.66	0.67

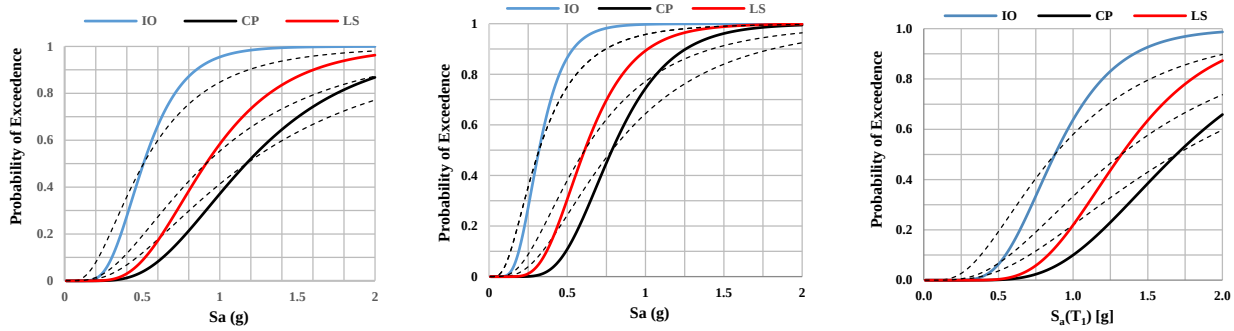

(a) (b) (c)

Fig. 14. Fragility curves of 3-story steel frame (a) with brace, (b) with infill and (c) combination of infill and brace

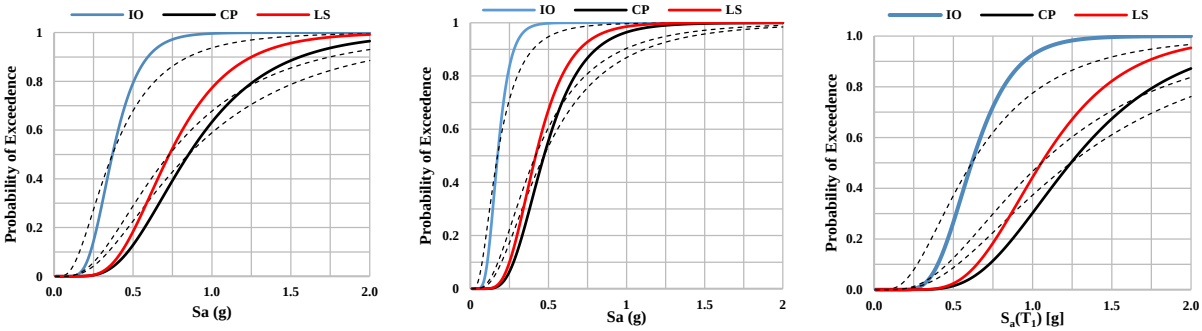

(a) (b) (c)

Fig. 15. Fragility curves of the 5-story steel frame (a) with brace, (b) with infill and (c) combination of infill and brace

4.4. Performance assessment

Based on PSHA results (Gholipour et al. [27]) for the area of interest, the spectral acceleration values at fundamental period of the buildings in addition to the probability of exceeding three considered performance objectives, for all model buildings considering two hazard levels are shown in Table 7. As it shows, the probability of exceeding all three

damage states are high reflecting high potential risks of these systems at future probable earthquakes. The frames with both infill panels and bracing perform better than the other two systems. Generally, infill walls in prototypes with shorter periods are improved structural performance in comparison with longer period models.

For frames with only infill walls, considerable higher damage probability is associated with 3-story and 5-story buildings due to the similar strength and stiffness of the infill walls in all floors and soft-story mechanism and lack of structural redundancy, as compared with braced structural systems. However, a high degree of damage is expected for all three performance levels as results indicated.

Table 7. Probability of exceeding performance level in 475 and 2475 hazard levels for considered buildings

No. Story	Lateral Load Resisting System	T_1	Probability of Exceedance (%) at 475 hazard level				Probability of Exceedance (%) at 2475 hazard level			
			S_{aT1}	IO	LS	CP	S_{aT1}	IO	LS	CP
3	Masonry Infill	0.302	0.86	93	70	55	1.87	99	94	90
	Bracing	0.294	0.86	79	46	33	1.87	97	85	74
	Combination of masonry infill and bracing	0.228	0.86	48	25	16	1.87	87	70	56
5	Masonry Infill	0.474	0.56	96	67	60	1.18	99	96	94
	Bracing	0.469	0.57	75	36	28	1.20	96	77	69
	Combination of masonry infill and bracing	0.368	0.74	61	29	22	1.52	92	71	62

5. Conclusions

Steel frame structures with semi-rigid saddle connections constitute a large number of existing buildings in urban areas in Iran. Such traditional systems have showed poor seismic performances as observed in past earthquakes. In this study, the results of some test experiments associated with the saddle connection and infill walls were incorporated into an analytical structural modeling in order to assess the seismic vulnerability of such structural systems in a probabilistic frame work. Both static nonlinear and incremental dynamic analysis procedures were utilized in the evaluation process for three conventional frame configurations with bracing elements, infill walls and the combination of bracings and infill walls. In creating fragility curves, the results obtained from IDA procedure were combined with those of a PSHA for a typical site located in Tehran, and the performance of each model were assessed at immediate occupancy (IO), life safety (LS) and collapse prevention (CP) performance limits.

Observing pushover and hysteretic curves, frames with infill walls only (without any bracing system) are very vulnerable due to the premature failure of the infills which result in sudden strength and stiffness degradation in the system. The corresponding hysteretic curves for such system is thin compared to braced frame with no infill walls. This system seems not

capable of resisting strong ground motions. In frames composed of both bracing elements and infill walls, lateral load resistant is relatively high. In these systems, two distinct phases are observable during seismic lateral response. First, before infills' failure, the system has a high amount of lateral strength and stiffness. In the second phase (after failure of infills), the only-source for lateral stiffness and strength of the system is provided by the bracing elements and a drop in strength and stiffness occurs. It is generally observed that infill walls provide strength and stiffness merely at the very early stage of response prior to their failure.

Results show that the performance of "saddle connection" structures with brace elements or the combination of infill walls and bracings are better than the case with infill walls only. More specifically studying the effect of infill walls, the performance enhancement is more notable in low-rise buildings (3-story) as compared to medium-rise buildings (5-story). Also, in frames with just infill walls, the formation of soft-story mechanism is observable in the first story. Thus, it is believed that strengthening of the lowest story in these structures is an appropriate way to enhance their seismic performance. The behavior of the braced frame with brick infills are better as compared to the braced frame structures.

The results of the fragility analysis show that for three-story frames with the combination of infill wall and bracing, for an earthquake scenario with a return period of 2475 years, the probability of exceeding IO, LS and CP levels are 87%, 70% and 56% respectively. These probabilities are 91%, 71% and 62% for five-story buildings noting that with the increase in the number of stories, the probability of exceeding specific damage levels has increased.

It seems that, generally, frames with semi-rigid saddle connections may not be safe for collapse prevention and also may not satisfy other performance levels in high seismicity sites. Therefore, it is believed that seismic retrofitting of such existing structures is quite essential.

References

[1] Iranian Population and Housing Census – Statistical Center of Iran (2006 census program), www.amar.org.ir; 2006.

[2] Amiri H, Aghakouchak AA, Shakib H. Performance assessment of steel braced frames with Saddle connections using capacity spectrum method. M.Sc. thesis, Department of Civil Engineering, Tarbiat Modares University, Tehran; 2004 [in Persian].

[3] Moghadam H. Earthquake Engineering, fundamentals and application, Tehran Farhang Pub; 2002, p. 547-582 [in Persian].

[4] Hosseini Hashemi B, Hassanzadeh M. Study of a semi-rigid steel braced building damaged in the Bam earthquake Journal of Constructional Steel Research 2008; (64) 704–721.

[5] FEMA 356. Prestandard and commentary for the seismic rehabilitation of buildings. Federal Emergency Management Agency, Washington, DC; 2000.

[6] Mazruei A, Mirghaderi M, Dehghani H. Experimental and theoretical study of Khorjini connection and presenting a new rigid connection, M.Sc. thesis. Iran: University of Tehran; 2000 [in Persian].

[7] Shakib H, Dardaei Joghan S, Pirizadeh M, Moghaddasi Musavi A. Seismic rehabilitation of semi-rigid steel framed buildings–A case study, Journal of Constructional Steel Research 2011; (67) 1042–1049.

[8] ATC-63, FEMA P695. Quantification of building seismic performance factors. Prepared by Applied Technology Council for Federal Emergency Management Agency, Washington, DC; 2009.

[9] Zea'ati A, Rafee'Pour AA. Damage investigation caused by Bam earthquake 2003 in public buildings. Kerman Management & Planning Organization, Kerman; 2003.

[10] Karami R, Moghadam H. Mechanical properties of Saddle connections. M.Sc. thesis, Department of Civil Engineering, Sharif Technical University, Tehran; 1991 [in Persian].

[11] Mazroui A, Mostafai H. Experimental investigation on new method of Saddle connections under cyclic loads, Journal of New Building Housing, Building Housing Research Center 1999; 4(2):2.

[12] Moghadam H, Aalaee SA. Evaluation of rotation capacity, behavioral characteristics and resistance of Saddle connections. 4th International Conference on Seismology and Earthquake Engineering, Tehran; 2003 [in Persian].

[13] Amiri H, Aghakouchak AA. Experimental Study of Cyclic Behavior Of conventional Saddle Kike Connections and Their Acceptance Criteria. Iranian Society of Steel Structures 2012; 7(9):79-96 [in Persian].

[14] Sadeghian P, Moghadam H. Investigating stiffness and strength of Saddle connections. Proceeding of 1th conference on Immunization and Retrofitting of Structures, Tehran; 2002 [in Persian].

[15] McKenna F, Fenves GL, Scott MH, Jeremic B. Open System for Earthquake Engineering Simulation (OpenSees). Pacific Earthquake Engineering Research Center, University of California, Berkeley, CA; 2000.

[16] Giuffre A. Pinto PE. Il Comportamento Del Cemento Armato Per Sollecitazioni Cicliche di Forte Intensita, Giornale del Genio Civile, Fascicolo 5, Istituto di Tecnica Delle Costruzioni, Facolta Di Architettura, Universita Degli Studi di Roma; 1970.

[17] Uriz P, Mahin SA. Toward earthquake resistant design of concentrically braced steel frame structures. PEER report 2008/08. Pacific Earthquake Engineering Research Center, University of California at Berkeley, Berkeley, CA; 2008.

[18] Ibarra LF, Medina RA, Krawinkler H. Hysteretic models that incorporate strength and stiffness deterioration. Earthquake Engineering and Structural Dynamics 2005; 34(12) 1489-1511.

[19] Mander JB, Nair B, Wojtkowski K. An experimental study on the seismic performance of brick-infilled steel frames with and without retrofit. Technical Report NCEER-93-

0001, National Center of Earthquake Engineering Research, State University of New York 1993; p. 1.1-3.1.

[20] Crisafulli F, Carr A, Park R. Analytical modelling of infilled frame structures – a general review. Bulletin of the New Zealand Society for Earthquake Engineering 2000; 33(1): 30-47

[21] Shing P, Mehrabi AB. Behaviour and analysis of masonry infilled frames. Progress in Structural Engineering and Materials 2002; 4(3):320-331.

[22] Farshchi HR, Moghadam AS. Experimental and Theoretical Studies on Cyclic Behavior of Braced Frame with Infill and without Infill. Journal of Seismology and Earthquake Engineering 2006; 9(4):202-220 [in Persian].

[23] Crisafulli FJ. Seismic behavior of reinforced concrete structures with masonry infills. Ph.D. Thesis, Department of Civil Engineering, University of Canterbury; 1997.

[24] Garivani S, Aghakouchak AA. Soltani MM. Effects of masonry infills on seismic behavior of steel frames with Saddle connections and their elements. Modares Civil Engineering Journal 2012; 1:p.55 [in Persian].

[25] Veshkini P, Aghakouchak AA. Experimental study of ductility of steel frames with Saddle connections. Modares Civil Engineering Journal (Scientific Research Quarterly) 2003; 14:15-27 [in Persian].

[26] Vamvatsikos D, Cornell CA. Incremental Dynamic Analysis. Earthquake Engineering and Structural Dynamics 2002; 31(3):491-514.

[27] Gholipour Y, Bozorgnia Y, Rahnama M, Berberian M, Ghoreishi M, Talebian N, Shaja-Taheri J, Shafeei A. Probabilistic seismic hazard analysis phase I – greater Tehran regions – Final report – University of Tehran; 2001.

[28] Shome N. Cornell A. Probabilistic seismic demand analysis of nonlinear structures. Report No. RMS-35, Department of Civil Engineering, Stanford University; 1999.

[29] FEMA 350. Recommended seismic design criteria for new steel moment frame buildings. Federal Emergency Management Agency, Washington, DC; 2000.

[30] HAZUS-MH. Multi-hazard Loss Estimation Methodology. Earthquake Model, HAZUS-MH MR1, Technical Manual, Washington, DC; 2003.

[31] Calvi GM, Bolognini D, Penna A. Seismic performance of masonry-infilled R.C. Frames: benefits of slight reinforcement. Congresso Nacional de Sismologia e Engenharia Sísmica, Guimarães; 2004.

[32] Braz-César MT, Oliveira D, Barros RC. Comparison of cyclic response of reinforced concrete infilled frames with experimental results. The 14th World Conference on Earthquake Engineering; 2008.

[33] Schneider SP, Zagers BR, Abrams, DP. Lateral strength of steel frames with masonry infills having large openings. Journal of Structural Engineering 1998; 124(8):896-904.